JCTC Journal of Chemical Theory and Computation

Phase-Dependent Photocatalytic Ability of TiO_2: A First-Principles Study

Hui Pan,*,† Baohua Gu,† and Zhenyu Zhang

Environmental Science Division, Material Science & Technology Division, Oak Ridge National Laboratory, Oak Ridge, Tennessee 37831, and Department of Physics and Astronomy, University of Tennessee, Knoxville, Tennessee 37996

Received May 25, 2009

Abstract: The electronic properties of defected TiO_2 were investigated using the first-principles calculations based on density functional theory and generalized gradient approximation. Three typical defects, oxygen vacancy, titanium interstitial, and titanium vacancy, were considered in three TiO_2 polymorphs, anatase, rutile, and brookite, respectively. Our calculations demonstrated that the defect band is formed by removing an oxygen atom from or inserting an interstitial Ti atom into the TiO_2 lattice, which is responsible for the improvement of photocatalytic ability due to the enhanced visible-light absorption. Our calculations further revealed that the defect formation energy increases as following brookite, anatase, and rutile, indicating that defects are easy to be created in brookite TiO_2. The relatively high defect density and wide defect band contribute to the better photocatalytic performance of brookite TiO_2 in visible light.

Introduction

Titanium dioxide (TiO_2) finds wide applications in pigment, photocatalyst, photovoltaic materials, gas sensor, electrical circuit varistor, biocompatible material for bone implants, and spacer material for magnetic spin valve systems.[1−4] TiO_2, as a photocatalyst, has attracted substantial interest and been widely studied since 1972.[5] The photocatalytic ability of TiO_2 strongly depends on the crystal structure, morphology, and size. TiO_2 has commonly three crystalline polymorphs: anatase, brookite, and rutile. Generally, the performance of anatase TiO_2 is recognized to be better than the rutile counterpart.[6−8] The photocatalytic performance of anatase TiO_2 was attributed to the shallow electronic levels induced by oxygen vacancy.[8] Recently, it has been illustrated that brookite TiO_2 is more electrochemically active than anatase TiO_2.[9−11] It has been argued that the defects, such as oxygen vacancy, may make a contribution to the photocatalytic ability,[12−14] because the defect, as a "local factor", interacts with the adsorbed molecules and allows effective charge transfer between the H_2O and the TiO_2 surface.[14,15] More recently, Wendt et al. reported that the defect state (Ti*3d*) in the bandgap of titania was attributed to Ti interstials and resulted in narrowing the bandgap,[16] which played a key role in providing the electronic charge required for O_2 adsorption and dissociation. To date, the mechanism for the phase-dependent photocatalytic ability has not been clarified. The understanding of the origin should help the searching of photocatalyst with high efficiency. In this work, we systematically studied the effects of the defects on the electronic properties of TiO_2 by first-principles calculations. The first-principles calculations confirmed that the defects whose states were located within the bandgap can result in the improvement of visible-light absorption and revealed the origin of the phase-dependent photocatalytic ability of TiO_2.

Methods

The first-principles calculation based on the density functional theory[17] and the Perdew-Burke-Eznerhof generalized gradient approximation (PBE-GGA)[18] was carried out to find the mechanism of the phase-dependent photocatalytic performance of TiO_2. The projector augmented wave (PAW) scheme[19,20] as incorporated in the Vienna *ab initio* simulation package (VASP)[21] was used in the study. The Monkhorst and Pack scheme of k point sampling was used for integration

* Corresponding author e-mail: panh@ihpc.a-star.edu.sg.
† Environmental Science.
‡ Material Science & Technology Divisions, ORNL.
§ University of Tennessee.

10.1021/ct9002724 CCC: $40.75
Published on Web 08/27/2009

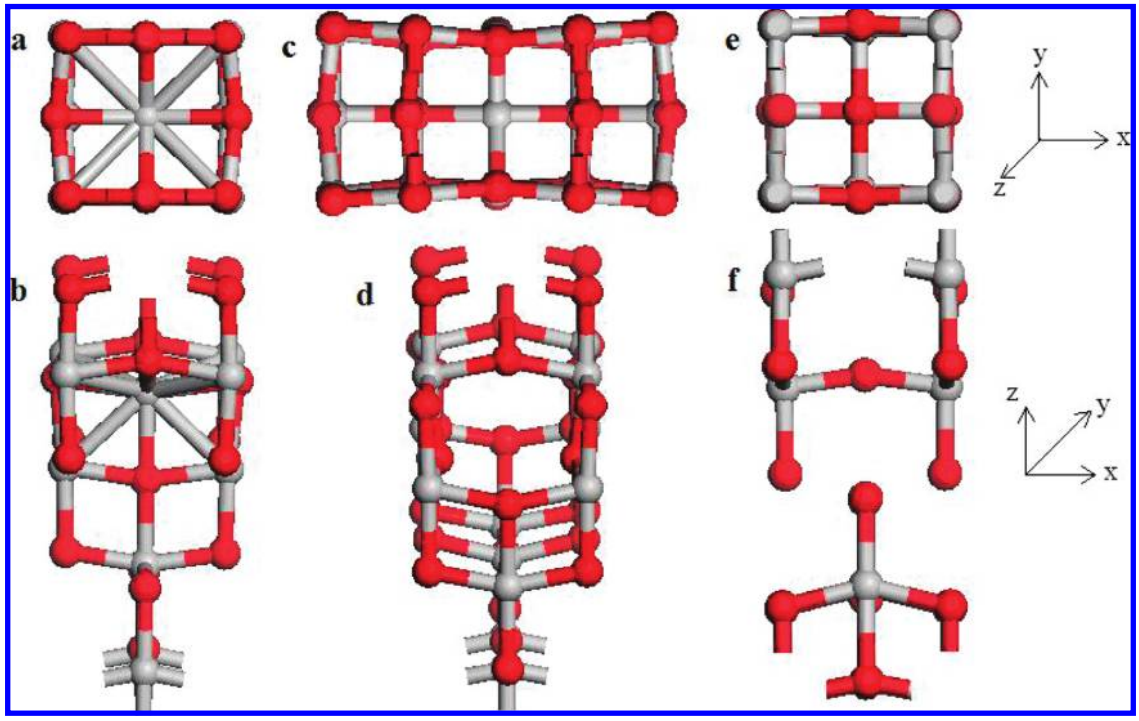

Figure 1. The local structures: (a) and (b) around Ti interstitial, (c) and (d) around oxygen vacancy, and (e) and (f) around Ti vacancy after geometry optimization.

over the first Brillouin zone.[22] The GGA+U method was used to treat *3d* electrons of Ti with the Hubbard on-site Coulomb interaction parameter (U-J) of 6 eV.[23] A $3 \times 3 \times 3$ grid for k-point sampling and an energy cutoff of 380 eV were consistently used in our calculations. Good convergence was obtained with these parameters, and the total energy was converged to 2.0×10^{-5} eV/atom. The bulk anatase, brookite, and rutile TiO_2 structures are modeled with a $3 \times 3 \times 1$, $1 \times 2 \times 2$, $2 \times 2 \times 3$ supercell containing 36 Ti atoms and 72 O atoms, 32 Ti atoms and 64 O atoms, 24 Ti atoms and 48 O atoms, respectively. The oxygen or titanium vacancy is modeled by removing oxygen or titanium atom from the supercell. The titanium interstitial is created by adding interstitial Ti atom into the supercell.

Results and Discussion

The local structure around the defect is distorted, such as bond extension, after geometry optimization. For anatase TiO_2 (a-TiO_2), the atoms surrounding the Ti interstitial (Ti_i) are pushed away with the change of the Ti−O bond length within 1.5% (Figure 1a,b). The effect of oxygen vacancy (V_O) on the local structure is different from that of Ti interstitial. V_O attracts the nearest Ti atoms and the oxygen atoms bonded with the Ti atoms in the x direction, while it pushes the oxygen atoms out in the y direction (Figure 1c,d). The change of the bond length in the local structure induced by V_O is within 1%. The Ti vacancy (V_{Ti}) slightly stretches the nearest oxygen atoms and Ti atoms (bonded with the nearest oxygen atoms) in all directions (Figures 1e,f) with a change of bond length within 0.5%. For brookite TiO_2 (b-TiO_2), the defect-induced distortion on the local structure is much less than that in a-TiO_2. The bond length around Ti_i is slightly extended within 0.5%, and the distortion induced by V_{Ti} or V_O is within 0.6%. The changes of bond length in the local structures of rutile TiO_2 (r-TiO_2) around Ti_i and V_O are within 1% and 0.5%, respectively. The Ti−O bond length in the local structure is reduced by 4% after removing one Ti atom from rutile TiO_2. The effect of Ti_i on the local structure decreases following a-TiO_2, r-TiO_2, and b-TiO_2.

The defects affect not only the local structure but also the electronic properties of TiO_2. Figure 2 shows the total and partial density of states (DOS and PDOS) of a-TiO_2 with and without defects. The calculated bandgap of perfect a-TiO_2 is about 2.72 eV (Figure 2a). The analysis of PDOS indicates that the valence top states and conduction bottom states of the perfect a-TiO_2 are mainly attributed to the oxygen *2p* states and Ti *3d* electrons, respectively (Figure 2b). For a-TiO_2 with a Ti interstitial, an intermediate band within the bandgap, defect states, can be observed in DOS of a-TiO_2 with Ti_i, which is close to the conduction band bottom (Figure 2c) and attributed to the interstitial Ti *3d* and oxygen (near the Ti_i) *2p* electrons (Figure 2d). The oxygen vacancy can also introduce an additional band into the bandgap, located almost at the middle of the bandgap (Figure 2e). The defect states induced by the oxygen vacancy are mainly attributed to the Ti *3d* electrons due to the unsaturated bonds after removing the oxygen atom (Figure 2f). The bandgap of a-TiO_2 is slightly reduced to 2.64 eV by removing the Ti atom from the lattice (Figure 2g). The Fermi level is within the valence band (Figure 2g), indicating that a-TiO_2 with V_{Ti} is a p-type semiconductor, consistent with the experimental reports.[14] The PDOS analysis indicated that the valence band top and conduction band bottom states of a-TiO_2 with V_{Ti} are mainly attributed to oxygen *2p* orbitals and Ti *3d* electrons, respectively (Figure 2h), similar to those of perfect a-TiO_2 (Figure 2b). For perfect r-TiO_2, the

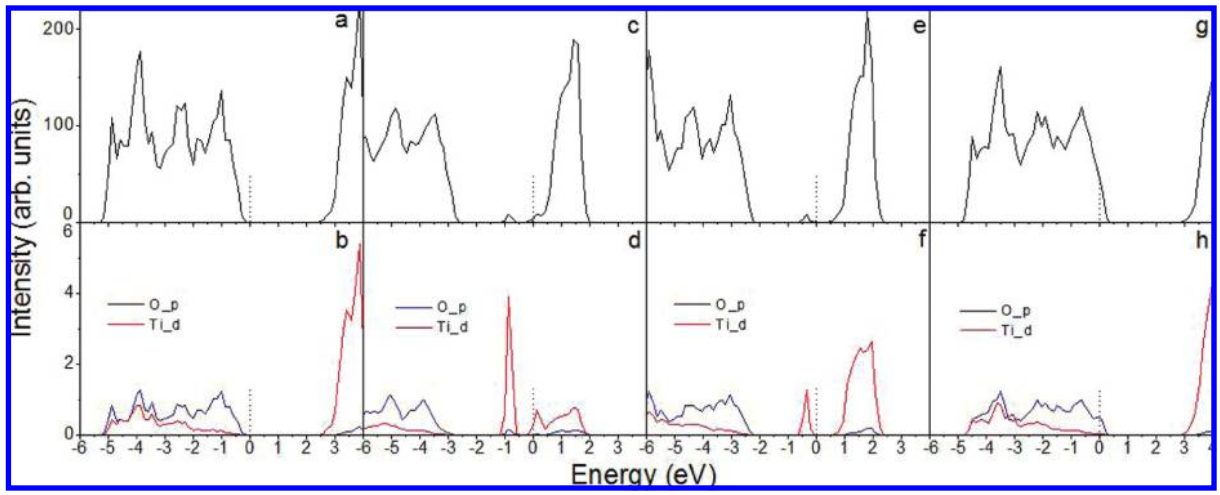

Figure 2. The calculated density of states (DOS) of a-TiO_2: (a) perfect, and with (b) Ti interstitial, (c) oxygen vacancy, and (d) Ti vacancy, and the calculated partial density of states (PDOS) of a-TiO_2 without defect (e) and with defect: (f) Ti interstitial, (g) oxygen vacancy, and (h) Ti vacancy.

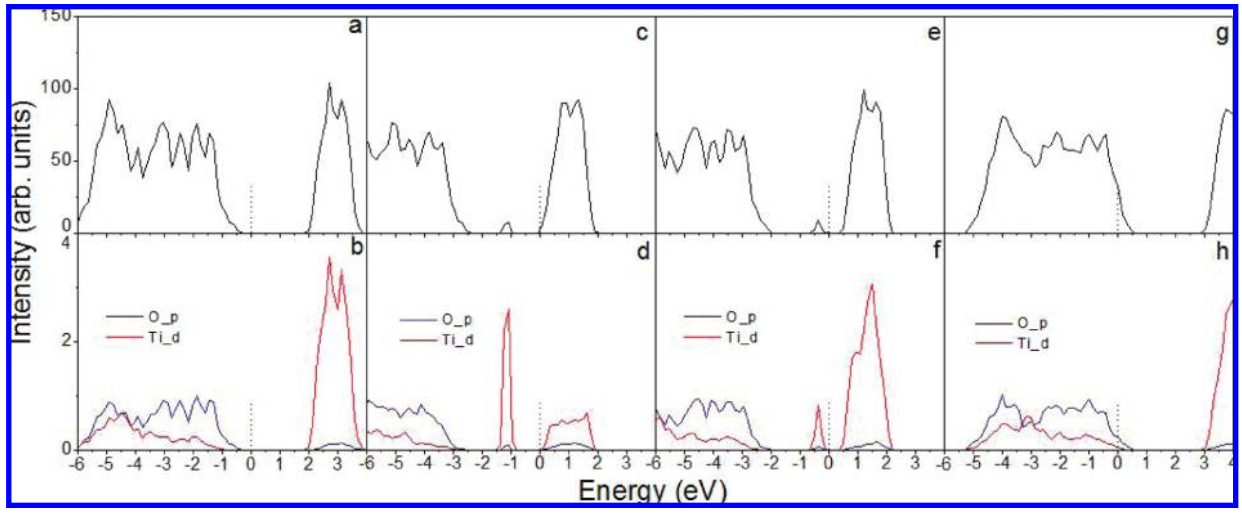

Figure 3. The DOS of r-TiO_2: (a) perfect, and with (b) Ti interstitial, (c) oxygen vacancy, and (d) Ti vacancy, and the PDOS of r-TiO_2 without defect (e) and with defect: (f) Ti interstitial, (g) oxygen vacancy, and (h) Ti vacancy.

calculated bandgap is 2.36 eV, as indicated in the DOS of r-TiO_2 (Figure 3a). The PDOS of perfect r-TiO_2 shows that the oxygen *2p* and Ti *3d* electrons are contributed to the valence top and conduction bottom states, respectively (Figure 3b). It was found that an intermediate band within the bandgap is formed by introducing Ti_i or V_O into the r-TiO_2 (Figure 3c,e) lattice, which is mainly attributed to Ti *3d* electrons (Figures 3d,f). The r-TiO_2 can also be a p-type semiconductor if removing a Ti atom from its supercell (Figure 3g). For perfect b-TiO_2, the calculated bandgap is 2.64 eV (Figure 4a), with its valence top and conduction bottom stated originating from the oxygen *2p* states and Ti *3d* electrons, respectively (Figure 4b). For defected b-TiO_2, similar results can be obtained. The Ti_i or V_O states form the intermediate band within the bandgap of b-TiO_2 (Figure 4c,e), mainly attributing to the Ti *3d* electrons (Figure 4d,f), and the V_{Ti} shifts the Fermi level down into the valence band (Figure 4g). Our calculations demonstrated that the intermediate band within the bandgap can be formed by creating V_O or Ti_i in the TiO_2 lattice, and the Fermi level is shifted into the valence band due to the formation of V_{Ti}, regardless of the crystal structure. However, it was found that the gap between the Ti_i defect band top and the conduction band bottom of b-TiO_2 (~0.12 eV, Figure 4c) (the PDOS shows that there is almost gapless between the defect and the conduction bands (Figure 4d)) is much less than those of a-TiO_2 (~0.57 eV, Figure 2c) and r-TiO_2 (1.0 eV, Figure 3c), and the Ti_i defect states occupy a width of ~0.61 eV in the bandgap of b-TiO_2, which may contribute to the better photocatalytic performance of b-TiO_2 due to the maximum absorption of sunlight induced by bandgap narrowing.

Figure 5 shows the formation energies of three-type defects in the three TiO_2 structures, which is estimated from

$$E_f = E_{tot}(TiO_2 + defect) - E_{tot}(TiO_2) + \mu_O(or \pm \mu_{Ti})$$

where $E_{tot}(TiO_2+defect)$ and $E_{tot}(TiO_2)$ are total energies of the TiO_2 with and without defect, respectively. μ_O and μ_{Ti} are the chemical potentials of O and Ti, respectively. $\mu_O = {}^1/_2\mu(O_2)$ and $\mu_{Ti} = \mu(Ti_{Bulk})$. The detailed numbers were provided in Table 1. We can see that the formation V_{Ti} requires higher energy than that of V_O or Ti_i, indicating V_{Ti}

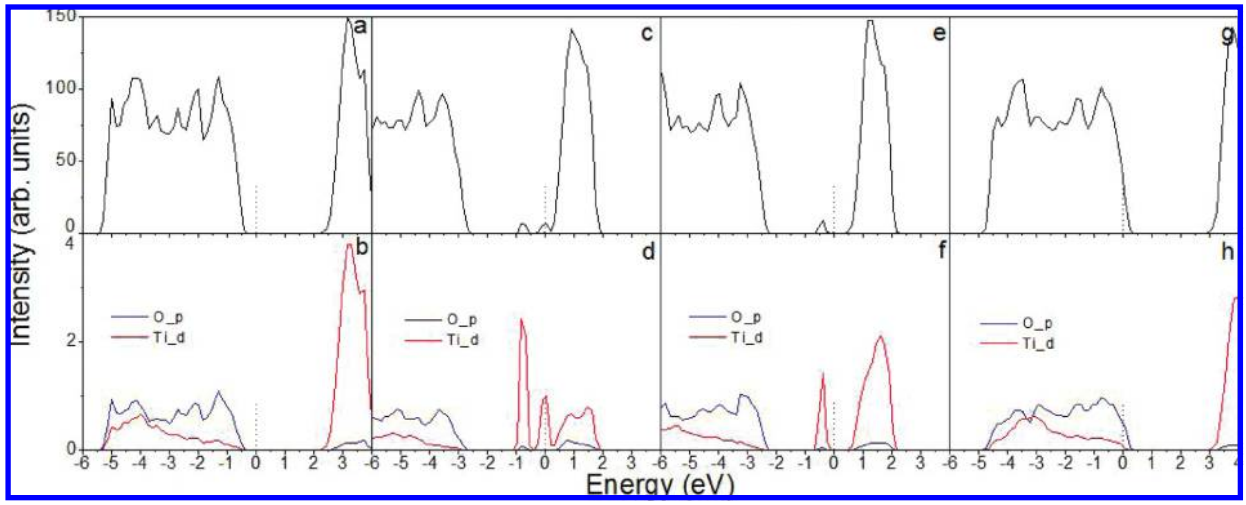

Figure 4. The DOS of b-TiO_2: (a) perfect, and with (b) Ti interstitial, (c) oxygen vacancy, and (d) Ti vacancy, and the PDOS of b-TiO_2 without defect (e) and with defect: (f) Ti interstitial, (g) oxygen vacancy, and (h) Ti vacancy.

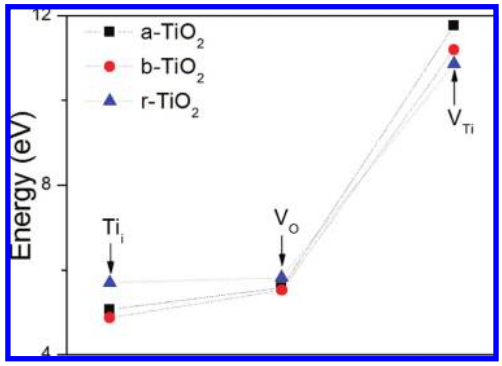

Figure 5. The formation energy of defect in the three TiO_2 structures.

Table 1. Calculated Formation Energies of Defects

	Ti_i (eV)	V_O (eV)	V_{Ti} (eV)
a-TiO2	5.07	5.58	11.76
b-TiO2	4.87	5.52	11.19
r-TiO2	5.70	5.82	10.86

is difficult to be created under moderate conditions. Experimentally, V_{Ti} can only be formed at elevated heating temperature and in oxygen ambiance,[14] consistent with our calculation results. The relatively low formation energies of V_O and Ti_i demonstrate the fact that TiO_2 is a nonstoichiometric compound with oxygen deficiency. Generally, the defect formation energy decreases with the trend of V_{Ti}, V_O, and Ti_i for the same TiO_2. The formation energies of V_{Ti} and V_O increase with the TiO_2 structures changing from brookite to anatase, further to rutile. The relatively low formation energy of Ti_i in b-TiO_2 indicates that its formation in b-TiO_2 is easier than that in a-TiO_2 and r-TiO_2, and b-TiO_2 may be produced under Ti-rich condition. In Ti-rich condition, the Ti interstitial is the dominant defect, which may trigger the formation of brookite structure due to its lower formation energy in b-TiO_2 (Figure 5).

From the calculated electronic properties of the defected TiO_2 and the defect formation energy, we may reveal the origin of the phase-dependent photocatalytic ability of TiO_2. The Ti_i and V_O are the most common defects in a-TiO_2 and r-TiO_2 due to their relatively low formation energies (Figure 5). However, the formation of Ti_i and V_O in a-TiO_2 is easier than those in r-TiO_2 because their formation energies in a-TiO_2 are less than those in r-TiO_2 (Figure 5). The relatively low formation energies of titanium interstitial and oxygen vacancy (E_f) in a-TiO_2 indicate that the defect density ($exp(-E_f/k_BT)$) is high, and the intermediate defect band within the bandgap induced by Ti_i or V_O in a-TiO_2 results in the maximally utilization of the sunlight (Figure 2), which should attribute to the improved photocatalytic performance of a-TiO_2. The observation of further improvement of photocatalytic ability in b-TiO_2 is also contributed to the easy formation of defects, increased defect density and enhanced light absorption. The relatively low formation energies of Ti_i and V_O in b-TiO_2 indicate that their densities are higher than those in a- and r-TiO_2. The defect states induced by the two-type defects may result in a broad defect band, even crossing the small gap and overlapping with the conduction band bottom (Figure 4c), i.e. the bandgap narrowing, similar to the doping effect. The defect-induced bandgap narrowing and the relatively high defect density due to lower defect formation energy in b-TiO_2 greatly enhance the photocatalytic performance of b-TiO_2 in visible light.

Conclusions

In summary, a systematic study of the defect effect on the photocatalytic ability of TiO_2 was carried out based on first-principles calculations. We found that the intermediate band induced by defect, Ti interstitial, or oxygen vacancy is located within the bandgap, responsible for the enhancement of visible-light absorption. The calculation on the defect formation energy indicated that titanium interstitial and oxygen vacancy are easy to be formed due to their lower formation energies. The formation energies of oxygen vacancy and Ti interstitial decrease as rutile, anatase, and brookite, revealing the mechanism of phase-dependent photocatalytic ability of TiO_2. The low formation energy of Ti interstitial in b-TiO_2 indicated that b-TiO_2 may be easily produced in Ti-rich condition. The better photocatalytic performance in b-TiO_2 in visible light is attributed to the

relatively high defect density, broad defect states in the bandgap, and bandgap narrowing.

Acknowledgment. This work was sponsored by the Office of Basic Energy Sciences, Division of Materials Sciences and Engineering and Laboratory Directed Research and Development (LDRD) Program of Oak Ridge National Laboratory (ORNL), which is managed by UT-Battelle LLC for the U.S. Department of Energy under contract No. DE-AC05-00OR22725. The DFT calculations were performed at the Computational Center of Science (CCS) of ORNL.

References

(1) Fujishima, A.; Hashimoto, K.; Watanabe, T. *TiO2 Photocatalysis. Fundamentals and applications*; BKC, Inc.: Tokyo, 1999; pp 14−176.

(2) Chen, X.; Mao, S. S. *Chem. Rev.* **2007**, *107*, 2891.

(3) Pfaff, G.; Reynders, P. *Chem. Rev.* **1999**, *99*, 1963.

(4) Linsebigler, A. L.; Lu, G.; Yates, J. T. *Chem. Rev.* **1995**, *95*, 735.

(5) Fujishima, A.; Honda, K. *Nature* **1972**, *238*, 37.

(6) Hoffmann, M. R.; Martin, S. T.; Choi, W.; Bahnemann, D. W. *Chem. Rev.* **1995**, *95*, 69.

(7) Hagfeldt, A.; Gratzel, M. *Chem. Rev.* **1995**, *95*, 49.

(8) Mattioli, G.; Filippone, F.; Alippi, P.; Bonapasta, A. A. *Phys. Rev. B* **2008**, *78*, 241201.

(9) Koelsch, M.; Cassaignon, S.; Guillemoles, J. F.; Jolivet, J. R. *Thin Solid Films* **2002**, *403*, 312.

(10) Shibata, T.; Irie, H.; Ohmori, M.; Nakajima, A.; Watanabe, T.; Hashimoto, K. *Phys. Chem. Chem. Phys.* **2004**, *6*, 1359.

(11) Iskandar, F.; Nandiyanto, A. B. D.; Yun, K. M.; Hogan, C. J., Jr.; Okuyama, K.; Biswas, P. *Adv. Mater.* **2007**, *19*, 1408.

(12) Lin, Z.; Orlov, A.; Lambert, R. M.; Payne, M. C. *J. Phys. Chem. B* **2005**, *109*, 20948.

(13) Serpone, N. *J. Phys. Chem. B* **2006**, *110*, 24287.

(14) Nowontny, M. K.; Sheppard, L. R.; Bak, T.; Nowontny, J. *J. Phys. Chem. C* **2008**, *112*, 5275.

(15) Nowontny, J.; Bak, T.; Nowontny, M. K. *J. Phys. Chem. B* **2006**, *110*, 21560.

(16) Wendt, S.; Sprunger, P. T.; Lira, E.; Madsen, G. K. H.; Li, Z.; Hansen, J. Ø.; Matthiesen, J.; Blekinge-Rasmussen, A.; Lægsgaars, E.; Hammer, B.; Besenbacger, F. *Science* **2008**, *320*, 1755.

(17) Hohenberg, P.; Kohn, W. *Phys. Rev.* **1964**, *136*, B864.

(18) Perdew, J. P.; Burke, K.; Ernzerhof, M. *Phys. Rev. Lett.* **1996**, *77*, 3865.

(19) Blöchl, P. E. *Phys. Rev. B* **1994**, *50*, 1795.

(20) Kresse, G.; Joubert, D. *Phys. Rev. B* **1999**, *59*, 1758.

(21) Kresse, G.; Furthmüller, J. *Phys. Rev. B* **1996**, *54*, 11169.

(22) Monkhorst, H. J.; Pack, J. D. *Phys. Rev. B* **1976**, *23*, 5188.

(23) Anisimov, V. I.; Aryasetiawan, F.; Lichtenstein, A. I. *J. Phys.: Condens. Matter* **1997**, *9*, 767.

CT9002724